

The variability of MAM rainfall over Southeast Ethiopia and its associated circulation features

Debelo Tamene^{1,2}, Yu Zhao¹, Vedaste Iyakaremye^{1,3} and Temesgen Gebremariam^{1,4}

¹Key Laboratory of Meteorological Disaster of Ministry of Education (KLME), Collaborative Innovation Center on Forecast and Evaluation of Meteorological Disasters (CIC-FEMD), International Joint Laboratory on Climate and Environment Change, Nanjing University of Information Science and Technology, Nanjing 210044, China

²Ministry of Agriculture Ethiopia, 6234 Addis Ababa, Ethiopian

³Rwanda Meteorology Agency, P.O. Box 898, Kigali, Rwanda

⁴Institute of Geophysics Space Science and Astronomy, Addis Ababa University, 1176, Addis Ababa, Ethiopia

*Corresponding Author: Yu Zhao, Nanjing University of Information Science and Technology, Nanjing 210044, China Tel: +95 9954 575 418; E-Mail: yuzhao@nuist.edu.cn

Received: February 16, 2021; Accepted: February 24, 2021; Published: February 26, 2021

Abstract

Previous studies investigated rainfall variability and its atmospheric features during June to September season that receives much of the rains in Ethiopia's Northern parts. Less attention was given to Ethiopia's southeastern part, which exhibits different rainfall regimes from the northern part. The present research uses CHIRPS and NCEP/NCAR reanalysis to analyze the Inter annual variability of March to May (MAM) seasonal rainfall and its associated circulation mechanisms over southeast Ethiopia from 1981 to 2019. The Empirical Orthogonal Function (EOF) is used to investigate the dominant modes in rainfall variability over the study area and identify typical wet and dry years later used for further analysis. The first three (3) eigenvectors (PC) explain 65% of the total variance. The composite analysis of wind anomalies shows that dry years were characterized by divergence at the low level (850hPa) and convergence at the upper level (200hPa). Wet years were dominated by convergence at a low level (850hPa) and divergence at the upper level (200hPa). The composite relative Humidity anomaly during wet years at a low level show that the entire study region is characterized by negative anomalies values, although it is not quite significant. The correlation analysis results indicated a positive correlation between Sea Surface Temperature (SST) and MAM seasonal rainfall total. This implies that the wet years are associated with warmer than normal SST over the identified regions except Tropical Indian, Western Pacific, and tropical Atlantic oceans. In contrast, the dry years are associated with cooler than normal over the same identified ocean regions. Further analysis shows a positive correlation between the Nino Index (3.4) and the MAM rainfall index over the study region with a correlation coefficient of 0.18. The findings of this study are helpful for agriculture planning and the prediction of MAM seasonal rainfall.

Keywords: Southeast Ethiopia; MAM; Belg; rainfall Variability; Seasonal

Introduction

Ethiopia is located in the Horn of Africa, within 3°-15°N, 33°- 48°E, has three climatological rainy seasons: June–September (called Kiremt), October–January (Bega), and February–May Belg; [1], And complex topography and with altitudes ranging from hundreds of meters below

Citation: Yu Zhao. The variability of MAM rainfall over Southeast Ethiopia and its associated circulation features, J Environ Sci. 2021; 17(2):183

© 2021 Trade Science Inc.

sea level in the northeast to over 4,000 m above sea level in the northern highlands [2]. The Ethiopian highlands are an essential factor for the rainfall pattern over Ethiopia [3]. In a country like Ethiopia, where irrigation schemes are not yet widely applied, the dependence of agriculture applied to seasonal rains is great. The agriculture sector and others like hydropower generation, water supply, and the like are highly controlled by seasonal rain performance [4]. For proper planning and avoiding risk, the county needs to know the rainy season's performance ahead of time.

Ethiopia has suffered from hazards connected to the high variability of rainfall and extreme climate events (MacLeod, 2019). Since the 1980s, the country continues to experience severe droughts and floods [5]. From 1990, Ethiopia recorded 47 major floods that killed approximately 2,000 people, and close to 2.2 million people were greatly affected [6]. In 2015, El Nino caused severe drought, which resulted in food insecurity among 10.2 million people.

The variability of rainfall in Ethiopia is determined mainly by the seasonal shift in large-scale circulation systems, which comprises the Inter tropical convergence zone (ITCZ) seasonal north to the south movement (Division et al., 2014). A recent study by [7] indicated that the rainfall is also linked to the warm equatorial central and eastern Pacific Ocean Sea Surface Temperatures (SSTs), which appear to cause the early JJAS onset but the shorter length of the season, while warm SSTs delay the JJAS cessation and cause prolonged rainfall in the Indian Ocean and Arabian Sea[7]. The movement and intensity of ITCZ vary from year to year, thus activating much of the Inter annual seasonal rainfall variability over the study domain. Apart from ITCZ and oceanic SSTs, the rainfall variability over Ethiopia is also linked to the El Niño Southern Oscillation (ENSO), which revealed that the boreal summer (JJAS) seasonal rainfall is known to cause El Nino failure. Several previous rainfall studies on the region have focused on the JJAS season that receives much of the rains in Ethiopia's Northern parts and its general circulation patterns. However, less attention was given to southeastern Ethiopia's region, which exhibits a different rainfall regime from the northern part. Therefore, for research and operational forecasting purposes, the teleconnection of southeastern rainfall variability with general circulation mechanisms need to be well investigated.

Rainfall prediction in Ethiopia is a challenge due to the observed inter-annual variability of used existing predictions [1]. Analyzing this variability of March-May (MAM) rainfall in Ethiopia can recommend the possible solution/precaution measures before the scenario. The majority of the research focuses on the south of Ethiopia, with little research conducted in Southeastern Ethiopia [8]. Therefore, this work aims to examine the following scientific questions. (1) Is there any rainfall belt shift during the March-May season from 1981-2019? (2) Is there any relationship between SST and MAM rainfall over Ethiopia? (3) Does Atmospheric circulation anomalies a source and cause of MAM rainfall variability over Ethiopia? It helps policymakers and stakeholders to mitigate the impact of seasonal forecasts in the agriculture, food security, water supply, and livestock sectors.

Study Area

It covers around 1.14 million square kilometers (944,000 square miles) country's topography comprises high and rugged plateaus and the peripheral lowlands, and the Elevations in the country range from 160 meters below sea level (northern exit of the Rift Valley) to over 4600 meters above sea level (of northern mountainous regions) [FIG.1].

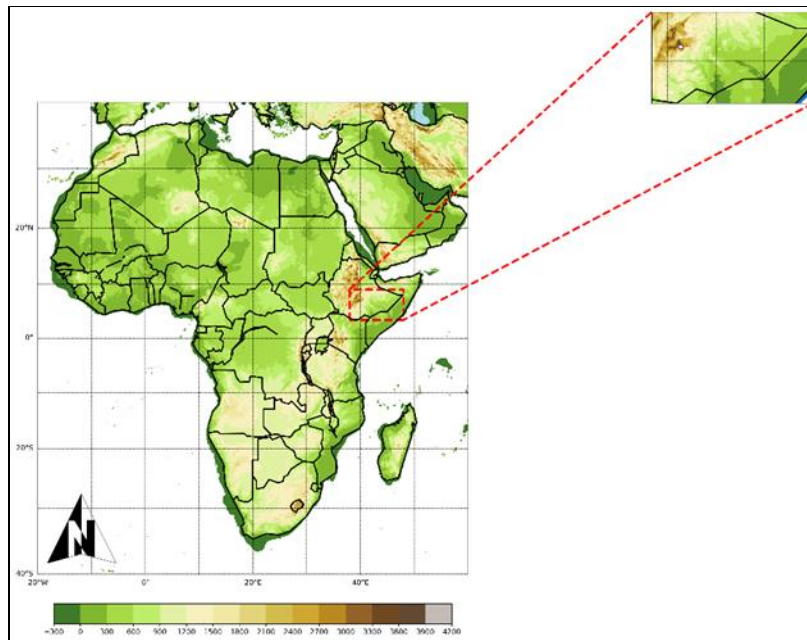


Figure 1: Geographical location of the study domain. The background color shows the elevation in km.

In terms of climate, Ethiopia is cold temperate on the plateau and hot in the lowlands. Furthermore, it lies wholly in the tropics, but its nearness to the equator is counter-balanced by an elevation of land, ranging from 2,200 to 2,600 m (7,218 to 8,530 ft.). The weather is usually wet and dry, but the MAM rains occur from February to April and the massive JJSA rains from mid-June to mid-September. The climate is extreme and high temperate. The area terrain in the lower basin of the Sobat is hot, swampy, and malarious. In the uplands, the air is cold in summer, and winter very dreary. The mean temperature ranges between 15°C to 25°C. On higher mountains, the climate is alpine.

Data and Method

Observational and Reanalysis datasets

Precipitation data from the Climate Hazards Group Infra-Red Precipitation with Station data (CHIRPSv2) is used to study rainfall variability over the study area. It incorporates multiple satellite imagery and in-situ station data to create rainfall to a 5 km resolution over the period from 1981 to 2019. The dataset has been used due to its high resolution and proved to represent Ethiopia's climate features [9]. It has also been used extensively over Africa, East Africa in particular.

The monthly Sea Surface Temperature dataset from The Hadley Centre Sea Ice and Sea Surface Temperature HadISST [10] was obtained to construct Nino3.4/3& IOD indices to analyze the correlation of the climatic drivers with SST. HadISST monthly SST has a resolution of 1°x 1°. For geo potential height, temperature, horizontal wind, vertical velocity, specific humidity at standard pressure levels, and mean sea level pressure (MSLP, hPa), the NCEP/NCAR reanalysis data sets were used NCEP/NCAR Reanalysis dataset has a horizontal spatial resolution of 2.5°x2.5°. These datasets were used to analyze the responses of atmospheric circulations and moisture transport to precipitation variability. The zonal and meridional wind components at 850hPa (the zone of low-level moisture advection) and 200hPa (maximum wind speeds level) were also used to analyze the relevant circulation patterns in wet and dry years.

Methods

A homogeneous target area was determined by analyzing the fraction of precipitation during the March-May season. The rainfall time series is the basis for statistical studies, including studying the regional climatic controls on Inter annual variability in the March-May season. Correlation, Composite Analysis, and Empirical Orthogonal Function were performed on the March-May rainfall time series and SST and atmospheric variables to examine linkages of precipitation with regional atmospheric circulation patterns SST anomalies.

Empirical Orthogonal Function (EOF) and correlation analysis

In this study, Empirical Orthogonal Function (EOF) analysis or Principal Component Analysis (PCA) technique [11] of seasonal precipitation was performed to demonstrate and extract the dominant modes of spatial homogeneity and noise of the precipitation. The eigenvector (V) in EOF analysis shows the spatial variability, whereas eigenvalues (Z) show the temporal patterns of seasonal rainfall in the matrix expression of EOF(X)X = V * Z . The PCA methods used to reduce a high-dimensional dataset into fewer dimensions while retaining important information. Moreover, this PCA clarifies the relationship between the seasonal trend (temporal pattern) and the inter-annual variation of the seasonal precipitation data, and the modes of temporal structures show the strength of seasonality.

To understand the influence of Tropical Indo-pacific seas surface temperature and associated climate drivers, the correlation between high seasonal percentage March-May precipitation anomalies with monthly climate indices SST were examined. The correlation coefficient, r_{xy} , is used to know a measure of the strength of the relationship between variables x and y for sample size n:

$$r_{xy} = \frac{\frac{1}{n} \sum_{t=1}^n (x_t - \bar{x})(y_t - \bar{y})}{\sqrt{\frac{1}{n} \sum_{t=1}^n (x_t - \bar{x})^2 \frac{1}{n} \sum_{t=1}^n (y_t - \bar{y})^2}} \quad (1)$$

Composite Analysis

The composite analysis is an essential technique to examine large-scale impacts of atmospheric circulation and tele connections on meteorological variabilities, like rainfall and SST [12]. So, we implemented a composite analysis technique to understand the impact of the tropical Indo-Pacific drivers [13] on February-May precipitation. Achieve composite analysis to the given phenomenon as mentioned by [14]; the first stage is choosing a means to define events for compositing. For example, to perform a composite analysis of this Nino3.4 region SST phenomenon, selecting a basis for the analysis positive basis to describe +Nino3.4 events, and the negative basis describes -Nino3.4 events come first. In the same fashion selecting basis of IOD events, the warming phase of IODW compared to IODE as a positive basis and vice versa is a negative basis. The next step is subtracting the average of the one basis from the other basis.

The statistical significance of the results will be determined using a 2-tailed Student t-test.

$$t = \frac{x_{mean} - y_{mean}}{\sqrt{\frac{(n_1 - 1)s_1^2 + (n_2 - 1)s_2^2}{n_1 + n_2 - 2} \sqrt{\frac{1}{n_1} + \frac{1}{n_2}}}} \quad (2)$$

where, x_{mean} and y_{mean} are the sample mean and s_2^2 & s_1^2 are the sample of variance. As well as $n_1 + n_2 - 2$ is the degree of freedom of the same sample size n_1 and n_2 .

Results and Discussions

Monthly and seasonal characteristics of rainfall over Southeast Ethiopia

[FIG. 2.] shows the spatial distribution of mean monthly rainfall (March-May) over southeast Ethiopia. From the figure, the wet season over Southeast Ethiopia can be identified as March, April, and May (MAM). During this period, much of the study region receives more rain compared to the other months. This MAM season is commonly known as Belg, and it's the primary source of rainfall for the water-scarce over South and Southeast Ethiopia. Generally, the country has experienced three distinct seasons, The Belg, Kiremt, and Baga season.

The seasonal patterns of rainfall in Ethiopia follow the Inter-Tropical Convergence Zone (ITCZ), which lags the overhead sun's seasonal migration (Nicholson, 2017). Rainfall association with ITCZ maintains bimodal over Southern Ethiopia and unimodal west-central Ethiopia, the northern part of Ethiopia's rainfall annual cycle. During MAM, the ITCZ moves slowly northwards, bringing heavy rainfall. A previous study showed Rainfall in Ethiopia is generally correlated with altitude, according to the Food and Agriculture Organization (FAO), 1984. There is substantially more rainfall in middle and higher altitudes (above 1,500 meters) than in the lowlands, except in the west, where rainfall is also high. Generally speaking, the mean annual rainfall level is greater than 900mm for areas above 1,500 meter.

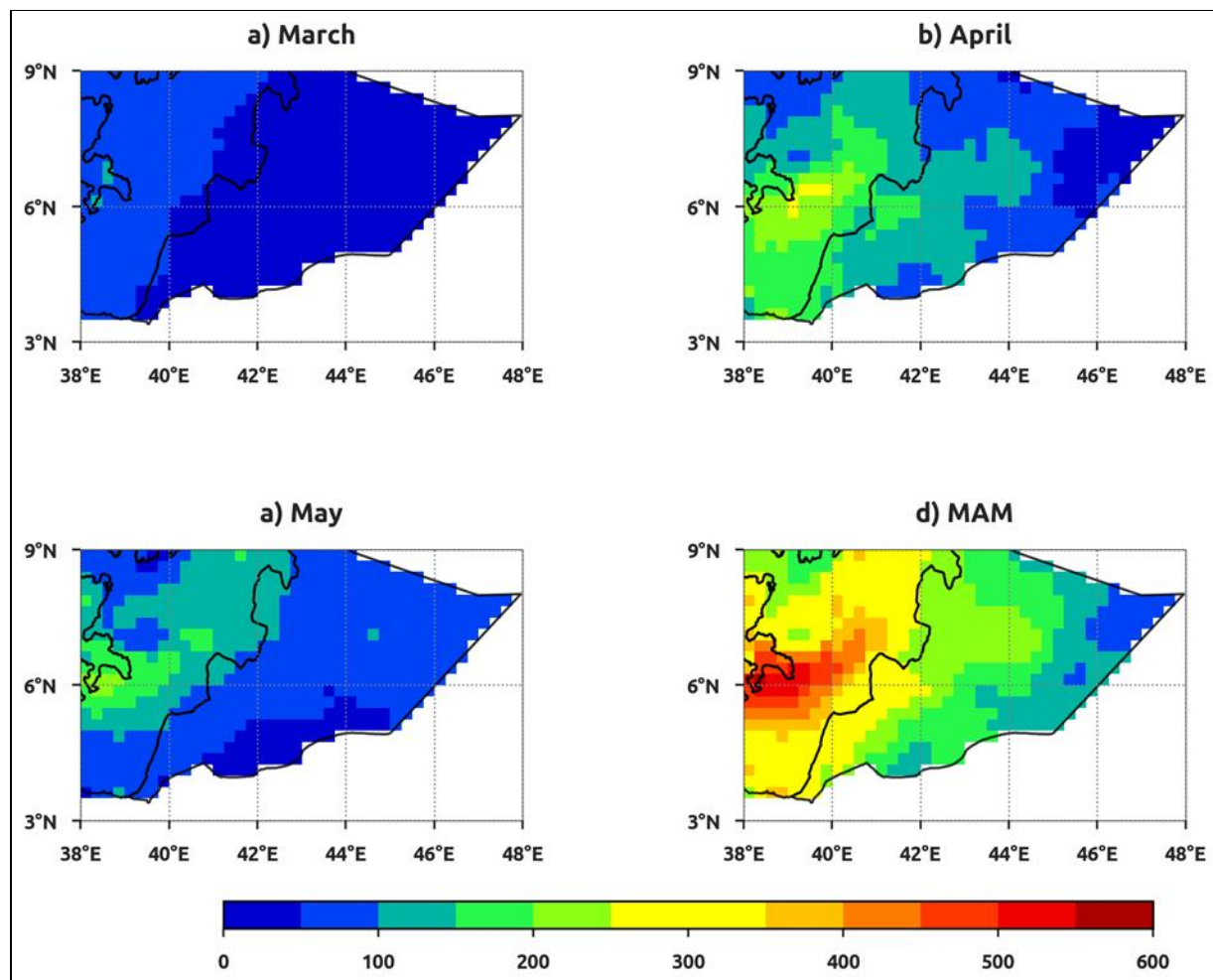


FIG. 2. Monthly mean precipitation (mm) and the total cumulative distribution over Southeastern Ethiopia for the period 1981-2019.

[FIG. 3.] shows the analysis of the MAM (Belg season) rainfall distribution. During the Belg season, the southern parts were captured to receive rainfall above 50% near or above-average rainfall. While the Northern parts receive below 40% of rainfall, the Southern parts receive

more rain during the MAM season than the Northern counterpart. There is mostly an interaction between the South easterlies and the coastal line because the Indian Ocean is warmer after February, bringing South easterlies inland, mostly towards Lake Victoria basins and Ethiopian highlands. Most of the spatial difference in rainfall is caused by elevation. Usually, a high altitude leads to too low temperature, as the average regional temperature decreases and altitude increases, as moist air rises, spreads, and cools, reaches its dew point (the temperature at which condensation takes place), produces a cloud, and ultimately falls as rain.

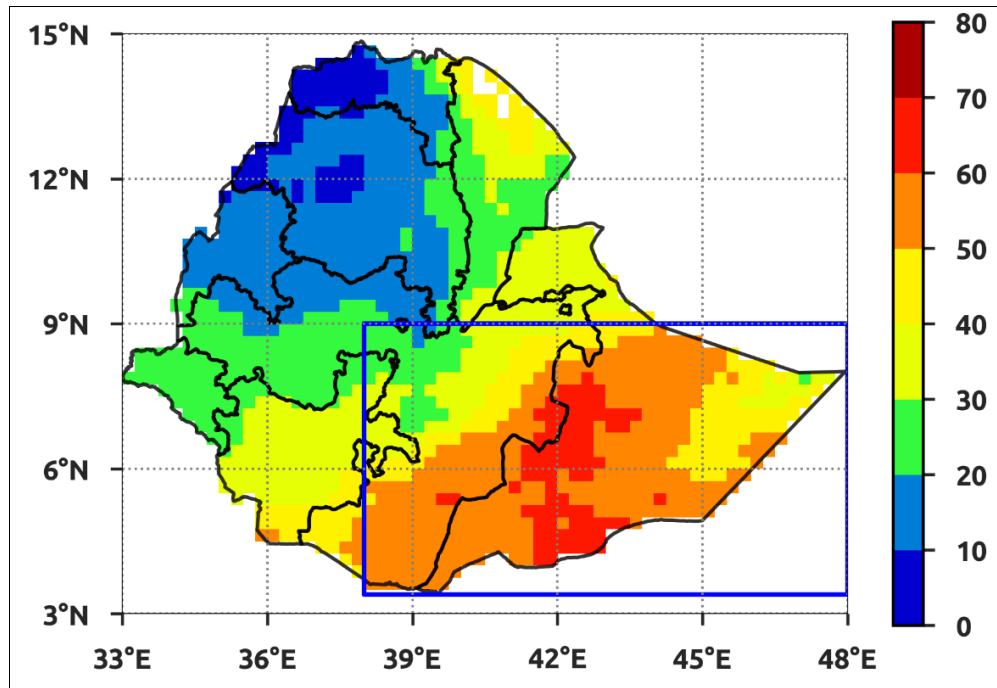


FIG.3. Seasonal fraction of annual rainfall for the March-May season. The blue box shows a spatial of seasonal rainfall greater than 50% of annual rainfall.

Temporal Distribution of rainfall climatology over the study area

Annual mean cycle rainfall: [FIG.4.] presents the time series of the annual mean rainfall over the southern parts of Ethiopia. The graph shows that the region experiences a pseudo-bimodal rainfall distribution pattern with the main season from March-May and the second season from July-November. The regions receive high rainfall amounts during April and May. However, the longest wet season captured in [FIG.4] is between June through November.

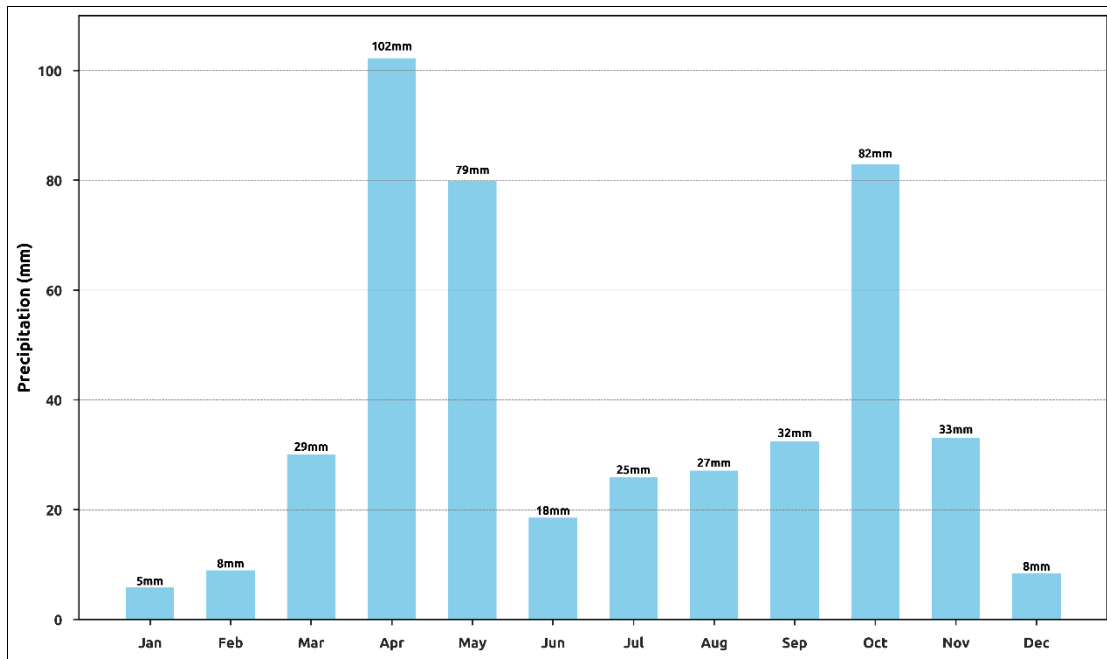


FIG.4. Monthly rainfall over (38°E- 48°E, 3°N-9°N), the blue box, as shown in Figure 3.

Long-Term Temporal Trends of seasonal (MAM) and annual rainfall: The long-term temporal trend of average rainfall over the study area was illustrated using linear regression and depicted in [FIG.5.]. The seasonal and annual series show high intra seasonal and Inter annual variations modulated by remote forcing. During MAM season, inconsistent temporal variability is accompanied by year-year fluctuation, and the rainfall amount is reducing at a frequency rate of 0.38 mm/Annun, as shown in [FIG.5a.]. The governing mechanism attributing to the Inter annual variability of MAM was associated with MJO with proportionate stability of Indo-Pacific SSTs inconsistency contributing to the decreasing rainfall gradient [15]; however, [FIG.5b.] shows, the annual variability pattern is different from the seasonal variation, it exhibits high Inter annual variability, and the rainfall amount is captured to be elevated at the frequency rate of 1.31mm/year since 1984.

The Inter annual variability during the MAM season is lesser than the annual; this is because of the ENSO influence, which is extensively consistent with a similar sign through the year yet feeble and conflicting amid the latter [16].

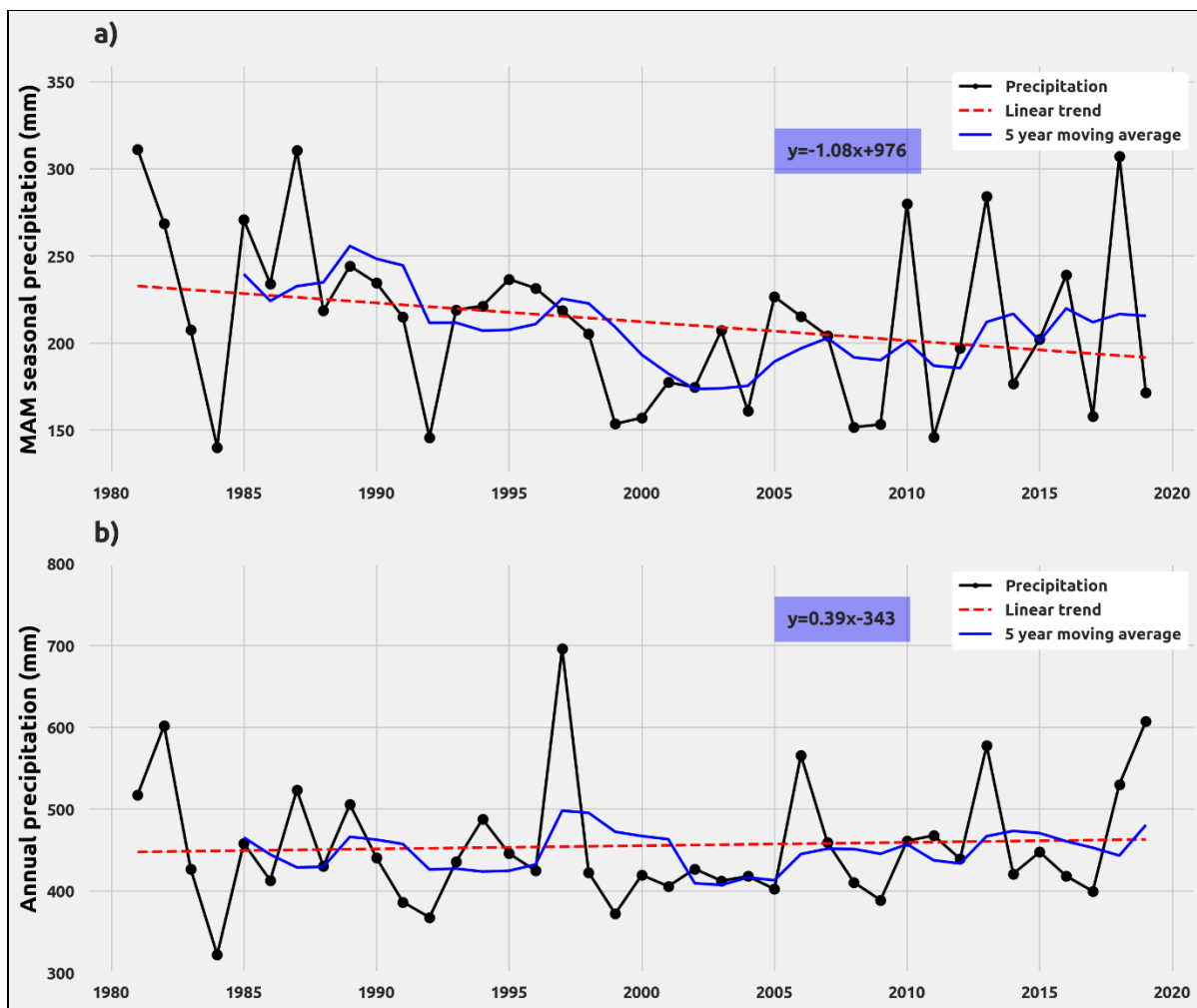


FIG. 5. Temporal variation of average precipitation during 1981–2019; (a) MAM, and (b) annual rainfall.

Inter annual Rainfall Variability: The Inter annual rainfall variability in [FIG.6.] of the mean MAM analysis captures the wet and dry events between 1981 and 2019. From [FIG.6.], precipitation over the study area exhibited high inter-annual variability. Wet years have been identified from the seasonal anomaly reaching more than 30% as 1987 and 2018. On the contrary, a dry year with a precipitation reduction of around -30% as 1984.

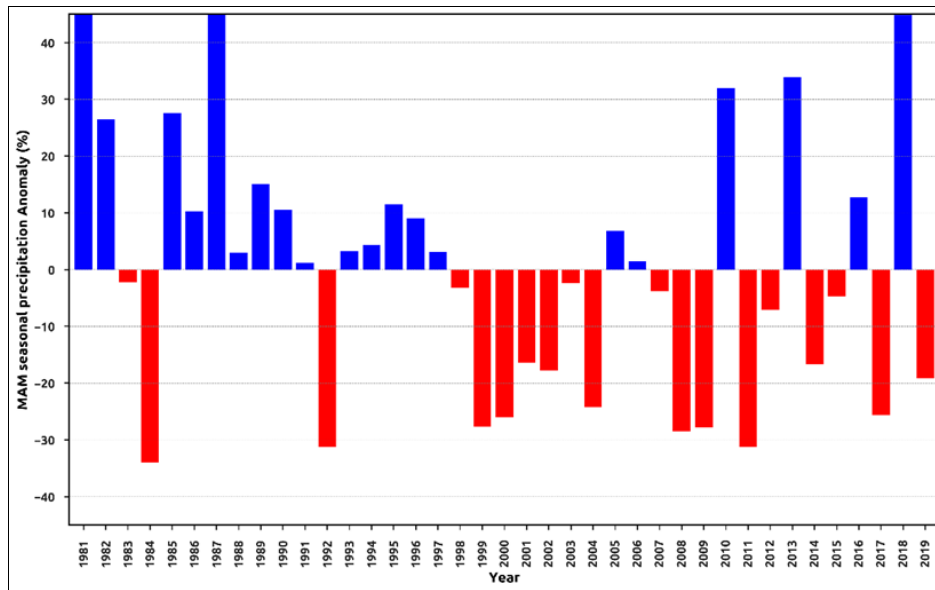


FIG.6. Line plot of the precipitation anomaly (in %) over southeast Ethiopia (38°E- 48°E, 3°N-9°N) for the period 1981-2019.

Empirical Orthogonal Function (EOF) Analysis

Dominant mode of Seasonal Precipitation: To examine the dominant modes of rainfall variability and Inter annual variability of MAM rainfall, EOF analysis was used to delineate homogeneous climate regions in southeast Ethiopia. Based on the criteria used by [11,17], a maximum of three EOF modes was found above the noise level. It may represent Great Horn Africa (GHA) rainfall variability for the March-May rainy season. The spatial (EOF 1, 2 and 3) components and their respective temporal (PCs) components are shown in [FIG.7.]. The first three leading components of EOFs (EOF1, EOF2, and EOF3) modes explain 39%, 17%, and 9% of the March-May total precipitation variance.

The first EOF [FIG.7a.] specifies a similar sign across the region, indicating that the leading EOF, which explains 39. % of the total variance is spatially homogenous, which confirms results in a spatial map of the March-May fraction of annual rainfall [FIG. 2]. Its corresponding PC1 is shown in [FIG.7b.]. It displays rainfall anomalies with the maximum values as wet years, such as; 1981, 1982, 1985, 1987, 2010, 2013, and 2018 and those with minimum values were considered as dry years, such as; 1984, 1992, 1999, 2000, 2008, 2009, and 2011 during the study period. The wet and dry years found in the leading PCA (PC1) were used for composite analysis.

The second mode, EOF2, and the corresponding principal component PC2 are shown in [FIG.7c] and [FIG.7d]. EOF2 displays a north/south dipole pattern. Its PC2 pattern in [FIG.7d.] shows that whenever negative rainfall anomalies occur over the Central and Western parts of Ethiopia, positive rainfall anomalies are experienced over the Southern parts, i.e., over the border Ethiopia and vice versa.

Similarly, the third mode, EOF3, and its corresponding principal component PC3 in [FIG.7e] and [FIG.7f] whereby the negative rainfall anomalies occurred over the Central extending to the country's Northern parts with positive rainfall anomalies experienced over the Southern parts and Western parts.

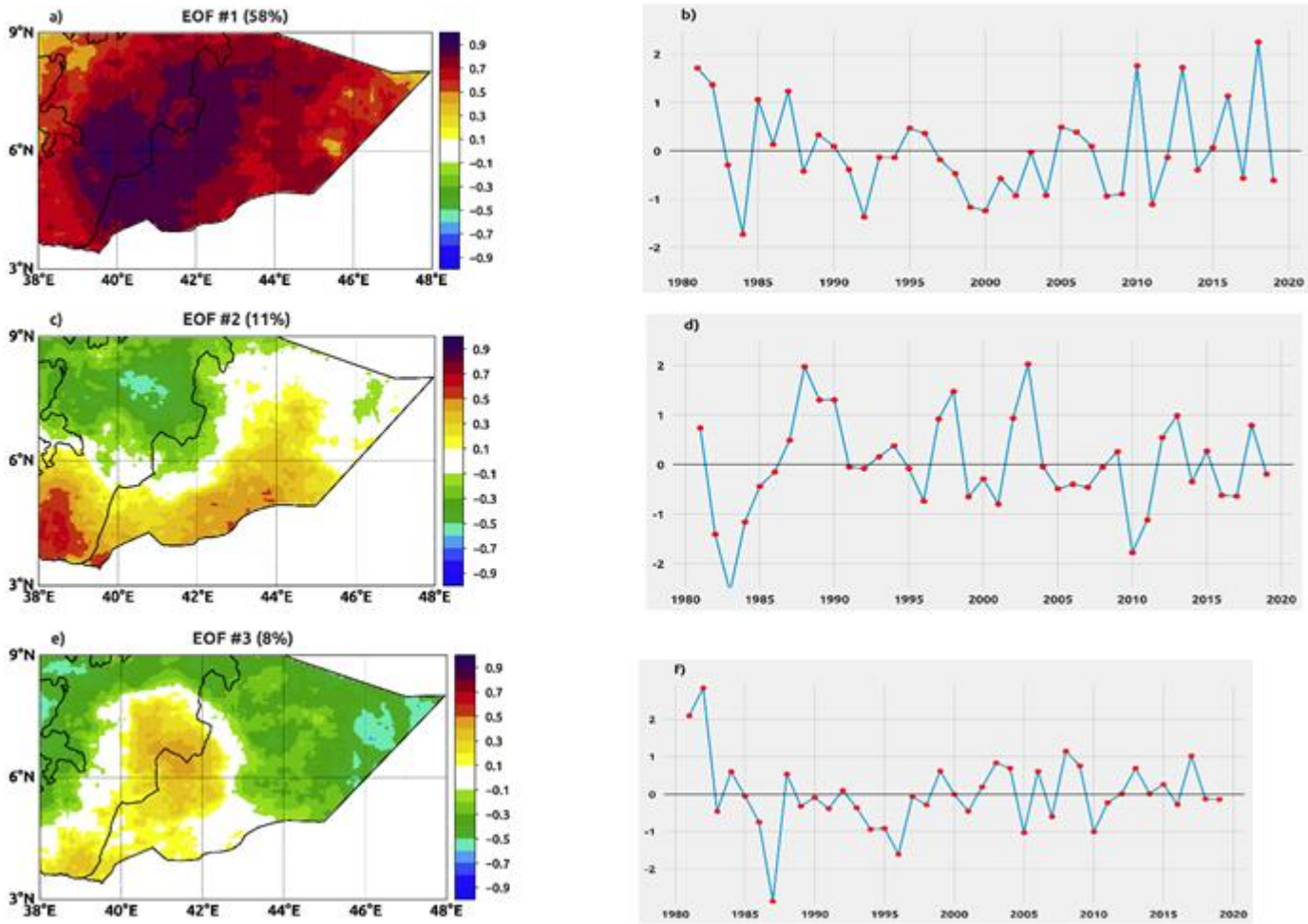


FIG.7. Spatial distribution of the first three EOF (as a correlation coefficient) of MAM seasonal anomalous precipitation over Southeast Ethiopia (left panels). The corresponding Principal components (right panels).

Circulation Anomalies Associated with Wet and Dry Seasons

Upper-Level Tropospheric Wind: A trough over the Red Sea at around 200hPa has been seen during the MAM rainy season. The trough pattern corresponds to an anomalous southerly extension over Northeast Africa of subtropical westerly jet streams (STWJ). STWJ, which is a relatively narrow and shallow stream of fast-flowing air with a maximum velocity of about 200hPa in the upper troposphere, is shown in [FIG.8]. [6] Found that the intensity of the Jet is strongest in the ridge and lowest in the troughs. This means that it is possible to treat the west of the trough as the jet exit, and thus the geostrophic component points to the high pressure, while the east of the trough can be taken as the jet entry, which means that the low pressure is pointed to by the geostrophic component. Therefore, the divergence area was ahead of the trough, which is likely to induce upward motion [17] and thus favorable to the precipitation. The STWJ is shifted to the north from its climatological during the dry years, and wet years are associated with an upper-level trough over Africa, which could be linked to the southward tilt of the STWJ.

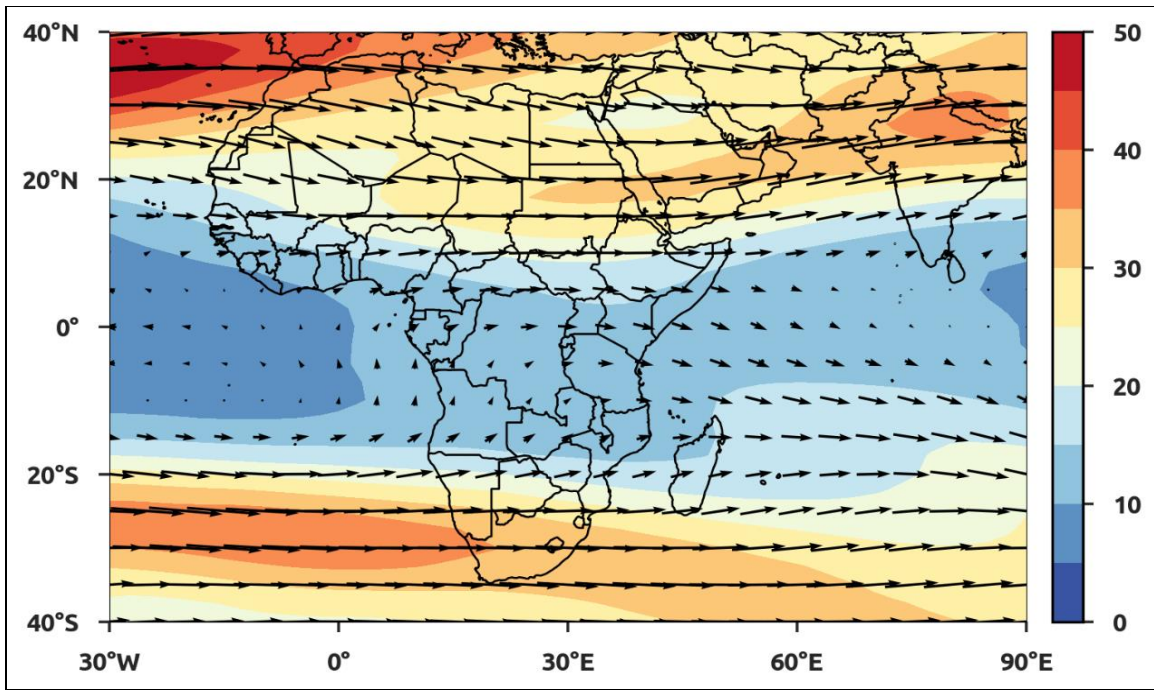
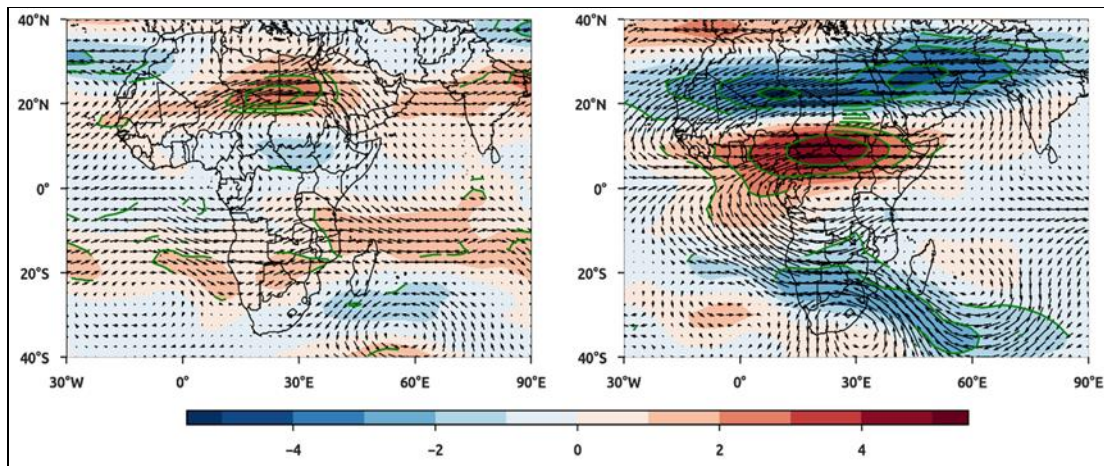


FIG.8. MAM wind climatology (1980-2019) at 200hPa. The colors represent the magnitude of the wind (m/s), and the arrows indicate the direction of the wind.

Upper-Level wind anomalies: An Investigation of the wind's circulation associated with EOF mode for dry and wet years was undertaken and analyzed. This was done to understand the wind flow and circulation pattern that prevailed over the study area during dry and wet years.

The upper level (200hPa) show that during dry years in [FIG.9a] there are negative winds anomaly over the study area and predominantly of North Easterly winds generated from the anti-cyclonic circulation over Central African which is favoring convective activity. This influences the weakening of the eastward flow over southeast Ethiopia in reducing the exported moisture away from Ethiopian highlands.



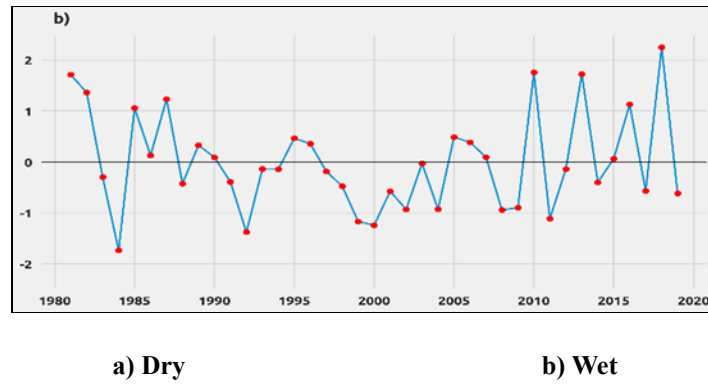


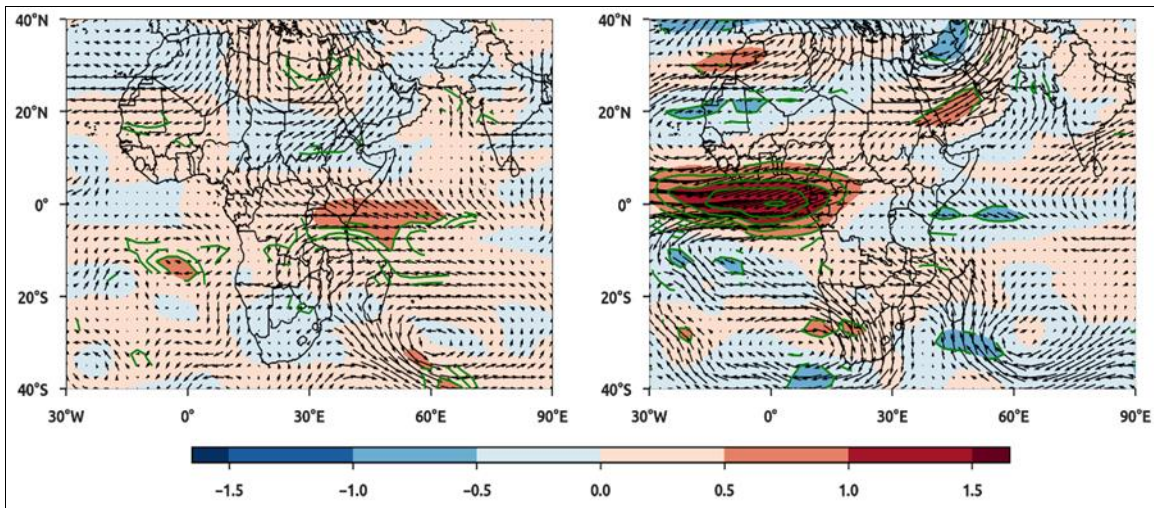
FIG.9. MAM composite wind anomalies during (a) dry years and (b) wet years at 200hPa, respectively. The arrow shows the wind anomaly's direction, and the colors represent the magnitude of the wind anomaly (m/s). Contour lines represent wind speed significant at 0.1 level.

FIG.9b. shows that wet years had a positive wind anomaly of high-speed westerly flow dominated the study region on the upper level (200hPa). During dry and wet years, these different wind directions indicate the wind source that contributed to the rainfall over the study area in terms of moisture transportation and cloud formation.

Low-Level Wind anomalies: Furthermore, results from the low-level winds (850hPa) for both dry and wet years in (FIG.10 a and b) explain the cross-equatorial component of flow towards East Africa, including the study area. Both the dry and wet tropospheric flow in the East African region indicates the significant effects of the land distribution in the tropics. During MAM season, the lower winds near the equatorial are mostly easterly rather than Westerly. This feature is consistent because the mean position of the upward branch of the Hadley circulation lies north of the Equator that influenced the study area. During composite dry years at the surface, [FIG.10a] reveals that the study region is dominated with negatively North Easterly wind anomalies advecting less moisture from the Arabian Peninsula in the Indian Ocean. A divergence circulation is located over the study area and did not effectively contribute moisture flux hence the recorded below normal rainfall. It is also noted that during dry years the study area was characterized by divergence at the lower level, which suppresses rainfall hence dry years. The westerly winds to the east of the Horn of Africa and southeasterly anomalies to the west of the Horn of Africa create the region an area of divergence if we consider the zonal (Walker) circulation in less rainfall.

Convergence at a low level leads to ascending motion, while divergence gives rise to vertical shrinking, suppressing convection due to subsidence [18,19].

During combined wet years at the surface in [FIG.10b], the results reveal a dominant Southeasterly from the Equatorial Indian Ocean and Westerly wind anomalies. These converging wind anomalies lead to moisture and increased convective activity, making the study region favorable to excess and significant rainfall. The wind anomalies at the low level during wet years are positively correlated with the Indian ocean includes over Southern areas of Ethiopia; this result marches with the observations made by [4] over the equatorial East Africa regions.



a) Dry

b) Wet

FIG.10. MAM composite wind anomalies during (a) dry years and (b) wet years at 850hPa, respectively. The arrows indicate the wind anomaly's course, and the colors reflect the wind anomaly's magnitude (m/s). Contour lines at a level of 0.1 reflect a substantial wind speed.

Relative Humidity Anomaly: [FIG.11.] represents the composite analysis of relative humidity (RH) anomaly during dry and wet years. This spatial display of the distribution of RH at a low level (850hPa) shows obtained results as depicted by (FIG. 11a and b); indicate that during dry years [FIG.11a], almost the entire study region is characterized by negative anomalies though it is not quite significant. This explains the suppressed rainfall activities experienced during the dry years. On the other hand, during wet years [FIG.11b], the study area is dominated by positive RH anomalies. This is because the area experienced much moist air that contributed to the conducive environment leading to more enhanced formation of rainfall activities.

The Northern and middle parts of the Indian Ocean were more Significant, while the West-Asia and far South of the Indian ocean gave negative anomalies of RH. That reflected a reasonable idea about connecting the likelihood of much rainfall with the relative humidity into the study area.

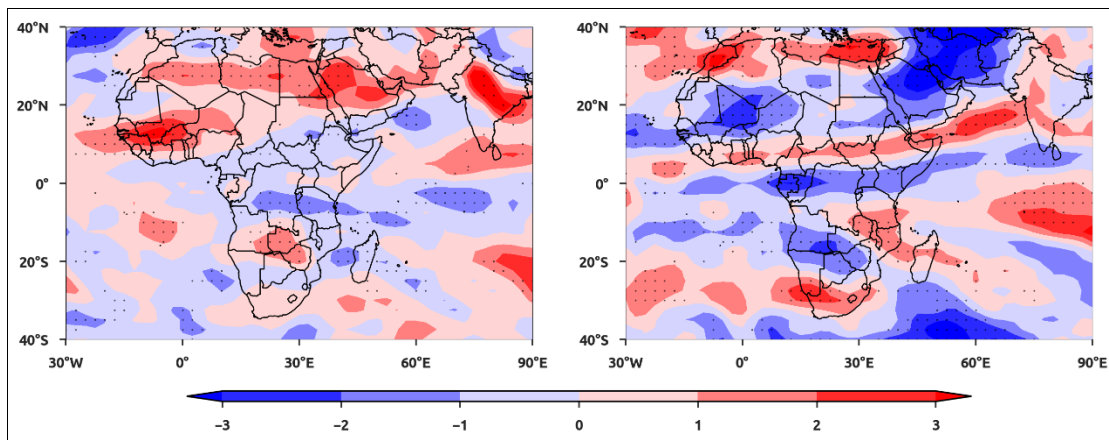


FIG.11. MAM relative humidity anomalies (unit: %) at 850 for (a) dry years and (b) wet years. Dots represent significant at 0.1 level.

Low-Level High Pressure: [FIG.12.] shows the composites of geo potential height at 850 hPa based on both dry years [FIG.12a] and wet years [FIG. 12b.]. The results suggested that there exists a strong signal that has been observed over extra tropical Atlantic and Pacific Oceans.

Dry years are associated with the positive North Atlantic Oscillation NAO relating to the negative anomaly around the Azores, and the wet years are associated with the negative.

There appears a positive anomaly over the Mascarene high system during dry years, which covers the Indian Ocean. The North Atlantic subtropical high shows similar results, with the negative anomaly dominating the Mediterranean. During wet years Siberian high pressure is captured positively, with negative significance covering the Indian Ocean. At the same time, negative anomalies dominated both the Northern and Southern Atlantic. The study area has shown significant positive anomaly in dry years and significant negative anomaly in wet years.

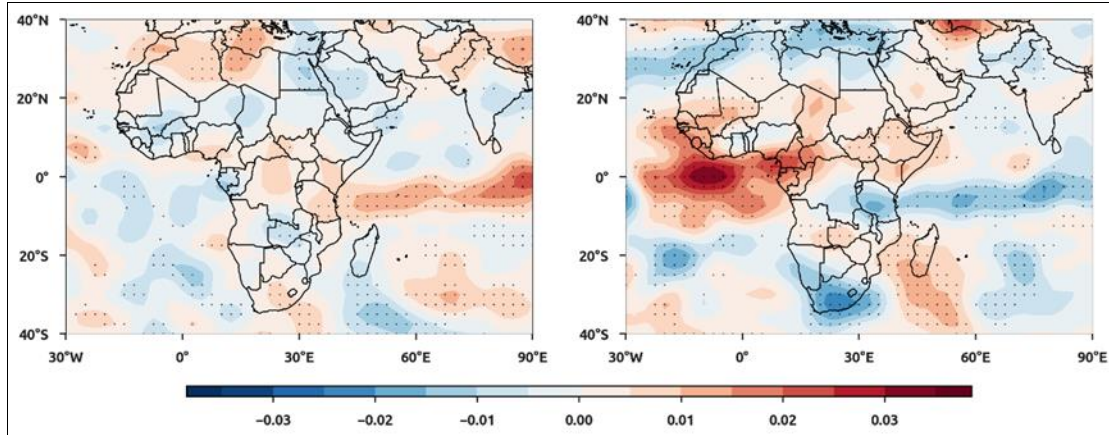


FIG.12. MAM composite of geopotential height anomalies during (a) dry years and (b) wet years at 850 hPa Dots represent significant at 0.1 level.

Sea Surface Temperature Anomaly: The Sea Surface Temperatures over the Pacific, Atlantic, and Indian tropical oceans are significant factors that influence Ethiopia's rainfall patterns (Southeastern parts). The results in (FIG. 13 a and b) show that combined dry years were associated with significant positive anomalies over the Indian and tropical eastern Pacific Ocean; on hand, strong negative anomalies were found over Mascarene high in the Indian equatorial Atlantic Ocean. Composite wet years were associated with strong positive anomalies over the tropical Indian, and the North and Southern Pacific Ocean of level 0.1 were obvious. In contrast, negative anomalies were observed over the Arabian Peninsula, west of the Indian Ocean, and tropical pacific (east of Australia). These situations of (SST) dominated the area of study in wet years.

This affirms that during El Niño years, southeast Ethiopia tends to experience above-normal rainfall, while during La Niña years, the region tends to experience below-average rainfall. Warm ENSO phase (El Niño). However, it is essential to note that ENSO episodes do not explicitly correlate with local conditions resulting in drought or floods over the study area. The regional and local conditions majorly control the climatic patterns, while ENSO may only serve to shift these conditions in one direction or another.

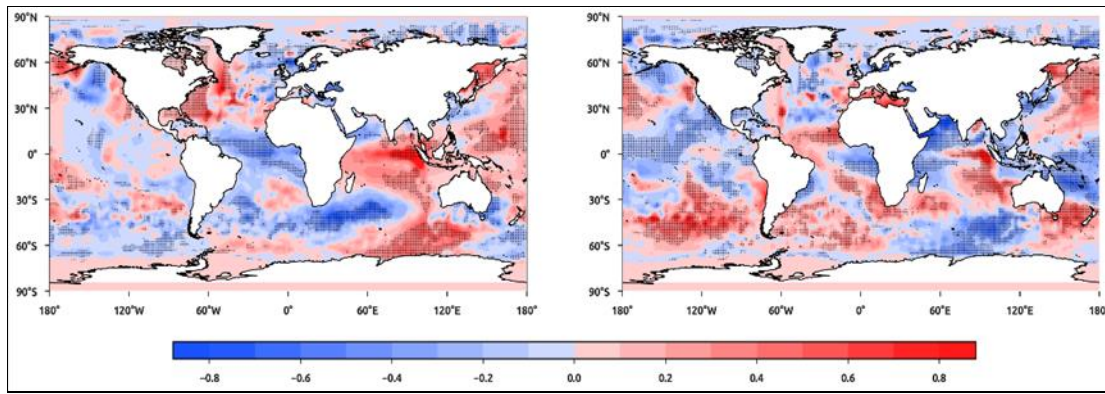


FIG.13. MAM composite global sea surface temperature anomaly patterns associated with PC1 during (a) dry years and (b) wet years Dots represent significant at 0.1 level.

Tele connections with Indian and Pacific Oceans: [FIG.14.] shows the tele connection analysis between MAM seasonal rainfall and global mean sea level pressure (MSLP). Results obtained reflect a significant negative relationship between the MAM rainfall and MSLP over the eastern Pacific, Indian and the tropical Atlantic Ocean over the study region. According to Ummenhofer et al. (2009), MSLP anomalies induce easterly onshore anomalies from the Indian Ocean and strengthens the westerly airflow across central Africa that joint over the coast equatorial East Africa. This view supports the results of our analysis.

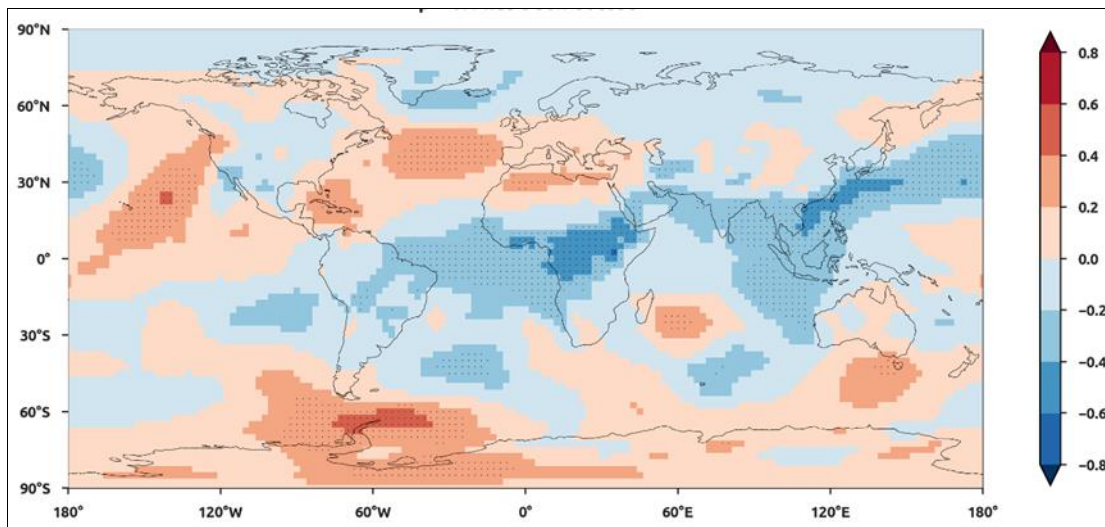


FIG.14. Correlation between MAM leading PCA and global sea level pressure (SLP). Dots represent significant at 0.1 levels.

ENSO Influence on MAM rainfall: Correlation patterns of MAM rainfall and global SST. Values $>+0.8$ and <-0.8 are shaded in brown and blue respectively. Brown Indicates a positive correlation, while blue indicates a negative correlation. The shaded regions are significant at 95% confidence level.

The tele connection of SST with the study regain shows a high positive correlation over Eastern and western tropical of the Pacific Ocean. This explains that ENSO influences the rainfall patterns over the region. The Northern Atlantic Ocean is observed to correlate positively with the study area, indicating the Northern Atlantic Oscillation (NAO) influence. Western Australia and the southern parts of the Indian ocean near Mascarenes high were also highly correlated with the study area. There exists a negative correlation between SST and the study during MAM rainfall over Tropical Indian, Western Pacific, and tropical Atlantic oceans.

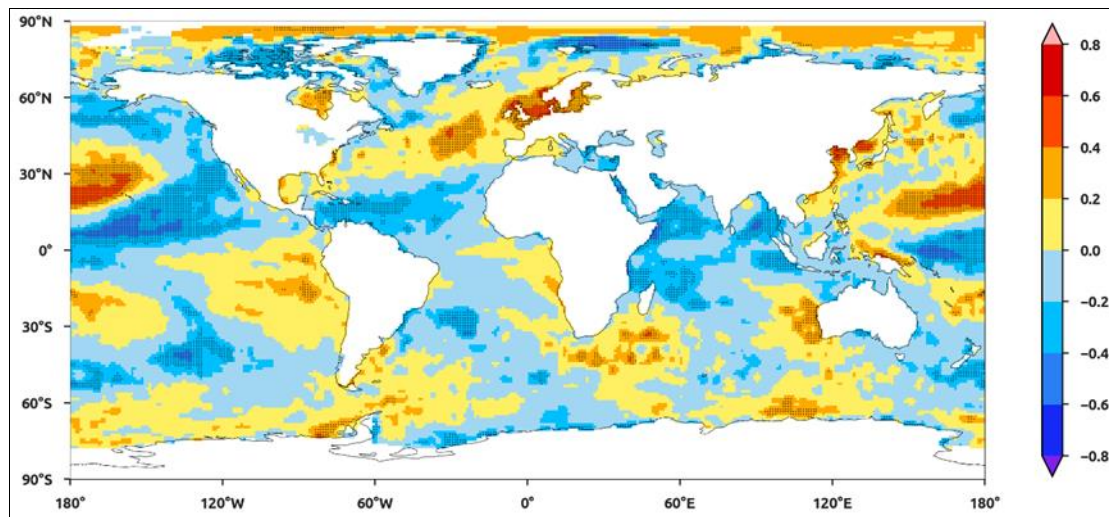


FIG.15. Correlation between MAM rainfall and sea surface temperature (SST). The dots represent significant at 0.1 level.

[FIG.16.] shows a positive correlation between the Niño Index (3.4) and MAM rainfall index over the study region with a correlation coefficient of 0.18. This indicates that more MAM rainfall is received in the years of the negative phase of SST over the central and eastern Pacific Ocean (generally EL Niño years), and less rainfall is recorded during La Niña Years. This agrees with Nicholas and Kim (1997). That the typical rainfall anomaly associated with ENSO is a dipole rainfall pattern: Eastern Africa is in phase with warm ENSO episodes, whereas Southern African is negatively correlated with these events. However, it showed that the higher the intensity of the Pacific Ocean's positive phase, the lower the MAM rainfall amounts received over Southeast Ethiopia. This implies that the southeast Ethiopian during cold ENSO (La Niña years) tend to receive less rainfall and the opposite occurs during the warm ENSO (El-Niño years) While summer rainfall is known to be influenced by the ENSO.

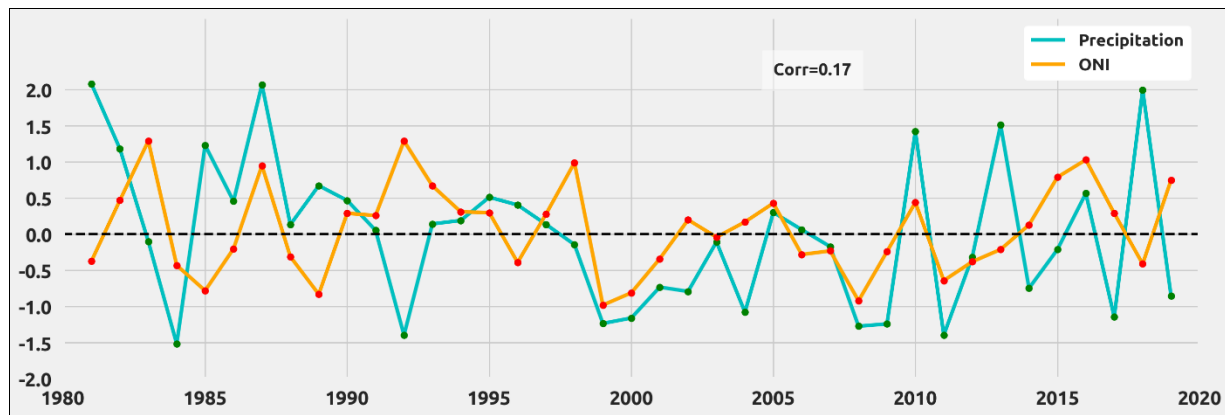


FIG.16. Relationship between MAM precipitation Index and Niño Index (3.4).

Conclusion

The study investigated the variability of MAM rainfall over Southeast Ethiopia and associated circulation mechanisms during 1981-2019. The analysis of both temporal and spatial variability in terms of rainfall distribution indicates that the country experiences a bimodal type of rainfall except for the Southeastern parts, which experience unimodal rains from March to May. The southeastern parts of Ethiopia receive the highest of its rains in April and May. The ITCZ movement influences the rainfall pattern, and it is associated with extreme weather events such as drought, Flash floods, and floods on an Inter annual timescale. The study used the Empirical Orthogonal Function (EOF) to investigate the dominant modes in rainfall variability over the study area and identify typical wet and dry years later used for further analysis.

The first three (3) eigenvectors (PC) explain 65% of the total variance—the composite analysis of various fields such as wind, relative humidity, and sea level pressure. Wind anomalies show that dry years were characterized by divergence at the low level (850hPa) and convergence at the upper level (200hPa). In contrast, wet years were dominated by convergence at a low level (850hPa) and divergence at the upper level (200hPa).

The composite relative Humidity anomaly during years at low-level show negative anomalies values characterizes the entire study region, although it is not quite significant. This explains the suppressed rainfall activities experienced during the dry years. On the other hand, the wet years were dominated by positive RH anomalies. This is because the area experienced much moist air that contributed to the conducive environment leading to more enhanced rainfall activities. The composite of Sea Surface Temperature showed dry years were associated with positive anomalies over the identified ocean regions. Strong negative anomalies were found over Mascarene high in the Indian and equatorial Atlantic Ocean. Wet years were associated with strong positive anomalies over the tropical Indian and the North and Southern Pacific Ocean. Negative anomalies were observed over the Arabian Peninsula, west of the Indian ocean, and tropical Pacific (east of Australia).

It has been seen from the correlation results That SST in the identified ocean regions was found to be highly positively correlated to the seasonal rainfall (MAM) over the study area. This implies that the wet years are associated with warmer than normal SST over the identified regions except Tropical Indian, Western Pacific, and tropical Atlantic oceans. The dry years are associated with cooler than normal over the same identified ocean regions. Further analysis shows a positive correlation between the Nino Index (3.4) and the MAM rainfall index over the study region with a correlation coefficient of 0.18. This means that in the years of the negative phase of SST over the central and eastern Pacific Ocean (usually EL Nino years), more MAM rainfall is obtained, and less rainfall is reported during the La Nina Years. This study's statistical analysis methods offered insights into the rainfall anomaly of the MAM associated with the large-scale mechanism. However, further work based on numerical simulations should be undertaken to understand the physical processes and dynamics responsible for the observed circulations patterns.

REFERENCES

1. Fekadu, K., Ethiopian Seasonal Rainfall Variability and Prediction Using Canonical Correlation Analysis (CCA). 2015. 4.112–119.
2. Gamachu, D. Some Patterns of Altitudinal Variation of Climatic Elements in the Mountainous Regions of Ethiopia. *Mt. Res. Dev.* 1988. 8, 131.
3. Degefu, M.A., Rowell, D.P., Bewket, W. Teleconnections between Ethiopian rainfall variability and global SSTs: observations and methods for model evaluation. *Meteorol. Atmos. Phys.* 2017.
4. Diro, G.T., Grimes. et.al. *African Climate and Climate Change.* 2011.
5. Tessema, I., Simane, B., Smallholder Farmers' perception and adaptation to climate variability and change in Fincha sub-basin of the Upper Blue Nile River Basin of Ethiopia. *GeoJournal.* 2020.7.
6. Satti, S., Zaitchik, B.F., Badr, H.S., Enhancing dynamical seasonal predictions through objective regionalization. *J. Appl. Meteorol. Climatol.* 2017. 56, 1431–1442.
7. Dubache, G., Ogwang, B.A., Ongoma, V., Towfiqul Islam, A.R.M., The effect of Indian Ocean on Ethiopian seasonal rainfall. *Meteorol. Atmos. Phys.* 2019.131, 1753–1761.
8. Jury, M., Climatic determinants of March-May rainfall variability over southeastern Ethiopia. *Clim. 2015. Res.* 66, 201–210.
9. Philip, S., Kew, S.F., van Oldenborgh. et.al., Attribution analysis of the Ethiopian drought of 2015. *J. Clim.* 2018.31, 2465–2486.
10. Kingdom, U., Agency, M., Kingdom, U., Information. et.al., A call for new approaches to quantifying biases in observations of

sea. 2017. 1601–1616.

11. Manatsa, D., Chipindu, B., Behera, S.K., Shifts in IOD and their impacts on association with East Africa rainfall. *Theor. Appl. Climatol.* 2012. 110, 115–128.
12. Wang C., Rasmussen B.P., Wynn K. Experimental comparison of energy-optimal coordinated control strategies for heat pump systems. *ASHRAE Trans.* 2017. 123, 162–173.
13. Preethi B., Sabin T.P., Adedoyin J.A. Impacts of the ENSO Modoki and other tropical indo-pacific climate-drivers on African rainfall. *Sci. Rep.* 2015. 5, 1–14.
14. Welhouse L.J., Lazzara M.A., Keller L.M., Composite analysis of the effects of ENSO events on Antarctica. *J. Clim.* 2016. 29, 1797–1808.
15. Nicholson, S.E. Climate and climatic variability of rainfall over eastern Africa. *Rev. Geophys.* 2017. 55, 590–635.
16. Kipkogei, O., Mwanthi, A.M., Mwesigwa, et.al., Improved seasonal prediction of rainfall over East Africa for application in agriculture: Statistical downscaling of CFSv2 and GFDL-FLOR. *J. Appl. Meteorol. Climatol.* 2017.
17. Nelson, W.A., *Statistical Methods, Encyclopedia of Ecology, Five-Volume Set.* 2008.
18. Ogowang, B.A., Guirong, T., Haishan, C. Diagnosis of September -November Drought and the Associated Circulation Anomalies Over Uganda. *Pakistan J. Meteorol.* 2012. 9, 11–24.
19. Barry, R.G., Chorley, R.J. *Atmosphere, weather and climate: Eighth edition, Atmosphere, Weather and Climate: Eighth Edition.* 2003.